Non-rigid image registration: theory and practice

W R CRUM, DPhil, T HARTKENS, PhD and D L G HILL, PhD

Division of Imaging Sciences, The Guy's, King's and St. Thomas' School of Medicine, London SE1 9RT, UK

Abstract. Image registration is an important enabling technology in medical image analysis. The current emphasis is on development and validation of application-specific non-rigid techniques, but there is already a plethora of techniques and terminology in use. In this paper we discuss the current state of the art of non-rigid registration to put on-going research in context and to highlight current and future clinical applications that might benefit from this technology. The philosophy and motivation underlying non-rigid registration is discussed and a guide to common terminology is presented. The core components of registration systems are described and outstanding issues of validity and validation are confronted.

Image registration is a key enabling technology in medical image analysis that has benefited from 20 years of development [1]. It is a process for determining the correspondence of features between images collected at different times or using different imaging modalities. The correspondences can be used to change the appearance – by rotating, translating, stretching etc. – of one image so it more closely resembles another so the pair can be directly compared, combined or analysed (Figure 1). The most intuitive use of registration is to correct for different patient positions between scans. Image registration is not an end in itself but adds value to images, *e.g.* by allowing structural (CT, MR, ultrasound) and functional (PET, SPECT, functional MRI (fMRI)) images to be viewed and analysed in the same coordinate system, and facilitates new uses of images, *e.g.* to monitor and quantify disease progression over time in the individual [2] or to build statistical models of structural variation in a population [3]. In some application areas image registration is now a core tool; for example (i) reliable analysis of fMRIs of the brain requires image registration to correct for small amounts of subject motion during imaging [4]; (ii) the widely used technique of voxel based morphometry makes use of image registration to bring brain images from tens or hundreds of subjects into a common coordinate system for analysis (so-called "spatial normalization") [5]; (iii) the analysis of perfusion images of the heart would not be possible without image registration to compensate for patient respiration [6]; and (iv) some of the latest MR image acquisition techniques incorporate image registration to correct for motion [7].

Historically, image-registration has been classified as being "rigid" (where images are assumed to be of objects that simply need to be rotated and translated with respect to one another to achieve correspondence) or "non-rigid" (where either through biological differences or image acquisition or both, correspondence between structures in two images cannot be achieved without some localized stretching of the images). Much of the early work in medical image registration was in registering brain images of the same subject acquired with different modalities (*e.g.* MRI and CT or PET) [8, 9]. For these applications a rigid

body approximation was sufficient as there is relatively little change in brain shape or position within the skull over the relatively short periods between scans. Today rigid registration is often extended to include affine registration, which includes scale factors and shears, and can partially correct for calibration differences across scanners or gross differences in scale between subjects. There have been several recent reviews that cover these
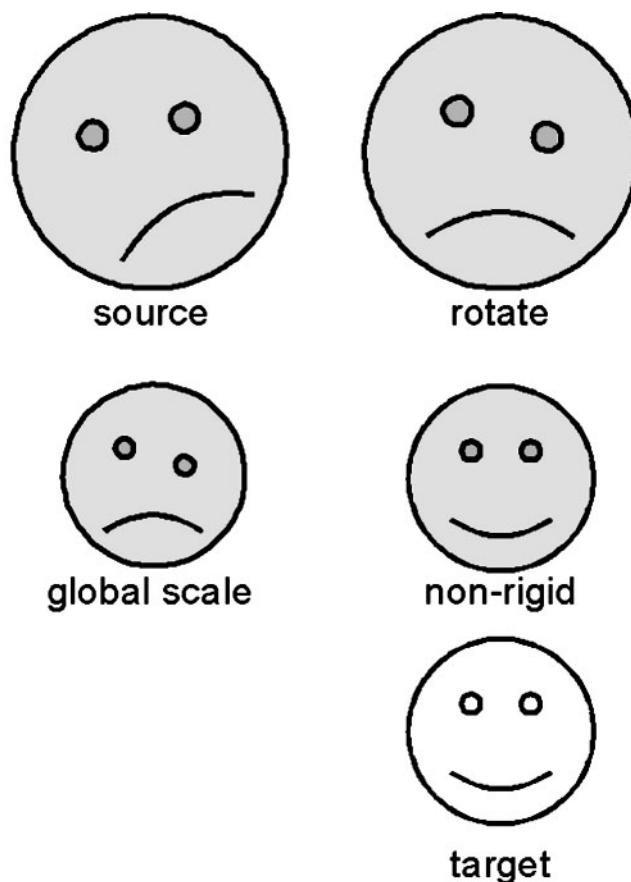

Figure 1. Schematic showing rigid and non-rigid registration. The source image is rotated, of a different size and contains different internal structure to the target. These differences are corrected by a series of steps with the global changes generally being determined before the local changes.

Address correspondence to Professor Derek Hill, Division of Imaging Sciences, Thomas Guy House (5th Floor), Guy's Hospital, London SE1 9RT, UK.

areas in more detail [1, 10]. Clearly most of the human body does not conform to a rigid or even an affine approximation [11] and much of the most interesting and challenging work in registration today involves the development of non-rigid registration techniques for applications ranging from correcting for soft-tissue deformation during imaging or surgery [12] through to modelling changes in neuroanatomy in the very old [13] and the very young [14]. In this paper we focus on these non-rigid registration algorithms and their applications. We first distinguish and compare geometry-based and voxel-based approaches, discuss outstanding problems of validity and validation and examine the confluence of registration, segmentation and statistical modelling. We concentrate on the concepts, common application areas and limitations of contemporary algorithms but provide references to the technical literature for the interested reader. With such broad ambition this paper will inevitably fail to be comprehensive but aims to provide a snapshot of the current state of the art with particular emphasis on clinical applications. For more specific aspects of image registration, the reader is referred to other reviews; there is good technical coverage in Hill et al [1], Brown [15], Lester and Arridge [16], Maintz and Viergever [17] and Zitova and Flusser [18], reviews of cardiac applications in Makela et al [19], nuclear medicine in Hutton et al [20], radiotherapy in Rosenman et al [21], digital subtraction angiography in Meijering et al [22] and brain applications in Toga and Thompson [23] and Thompson et al [24].

Registration and correspondence

Image registration is about determining a spatial transformation – or mapping – that relates positions in one image, to corresponding positions in one or more other images. The meaning of correspondence is crucial; depending on the application, the user may be interested in structural correspondence (*e.g.* lining up the same anatomical structures before and after treatment to detect response), functional correspondence (*e.g.* lining up functionally equivalent regions of the brains of a group of subjects) or structural–functional correspondence (*e.g.* correctly positioning functional information on a structural image). A particular registration algorithm will determine correspondence at a particular scale, and even if this transformation is error-free, there will be errors of correspondence at finer scales. Sometimes the scale is set explicitly; in registration using free-form deformations [25] the displacements of a regular grid of control-points are the parameters to be deduced and the initial millimetre spacing between these points defines a scale for the registration. In some other registration types the scale-selection is more implicit; in the registration used in the statistical parametric mapping (SPM) package (http://www.fil.ion.ucl.ac.uk/spm/) for example the number of discrete-cosine basis functions must be specified by the user with higher numbers introducing more flexibility into the registration and hence the ability to determine correspondences at a finer scale [5]. It is worth emphasising that increased flexibility comes at some cost. The most obvious penalty is that more parameter determination tends to mean more computer time is required. Rigid and affine registrations can typically be determined in seconds

or minutes but most non-rigid registration algorithms require minutes or hours with that time being spent either identifying a geometric set of corresponding features to match directly (see below) or automatically determining a large number of parameters by matching voxel intensities directly. Another issue is that typically the transformation is asymmetric: although there will be a vector that, at the scale of the transformation, describes how to displace each point in the source image to find the corresponding location in the target image, there is no guarantee that, at the same scale, each point in the target image can be related to a corresponding position in the source image (see Appendix 1 for a description of common terminology such as source and target). There may be gaps in the target image where correspondence is not defined at the selected scale. Some work has been done on symmetric schemes which guarantee the same result whether image A is matched to image B or vice versa [26]. This may be more appropriate for some applications (matching one normal brain to another) than others (monitoring the growth of a lesion). Finally, there is the question of redundancy. If geometrical features are used to match images then there will be many different possible deformation fields which can align those features but which behave differently away from those features or may be constrained in some way (*e.g.* to disallow situations where features can be "folded" to improve the image match but in a non-physical way). Similarly there will also be many possible deformation fields that can result in voxel intensities appearing to be well matched between images. With all these possibilities how do we distinguish between equivalent fields and how do we know what is "right" for a particular application? These are issues of current importance [27] and are discussed in the context of validation below.

Components of registration algorithms

A registration algorithm can be decomposed into three components:

- the similarity measure of how well two images match;
- the transformation model, which specifies the way in which the source image can be changed to match the target. A number of numerical parameters specify a particular instance of the transformation;
- the optimization process that varies the parameters of the transformation model to maximize the matching criterion.

Similarity measures

Registration based on patient image content can be divided into geometric approaches and intensity approaches. Geometric approaches build explicit models of identifiable anatomical elements in each image. These elements typically include functionally important surfaces, curves and point landmarks that can be matched with their counterparts in the second image. These correspondences define the transformation from one image to the other. The use of such structural information ensures that the mapping has biological validity and allows the

transformation to be interpreted in terms of the underlying anatomy or physiology.

Corresponding point landmarks can be used for registration [28] provided landmarks can be reliably identified in both images. Landmarks can either be defined anatomically (*e.g.* prominences of the ventricular system), or geometrically [29–32] by analysing how voxel intensity varies across an image. When landmarks are identified manually, it is important to incorporate measures of location accuracy into the registration [28]. After establishing explicit correspondences between the pairs of point landmarks, interpolation is used to infer correspondence throughout the rest of the image volume in a way consistent with the matched landmarks. Recent work has incorporated information about the local orientation of contours at landmark points to further constrain the registration [33]. In other studies, linear features called ridges or crest lines are extracted directly from three-dimensional (3D) images [30, 34–36], and non-rigidly matched. Then, as above, interpolation extends the correspondences between lines to the rest of the volume. For some anatomy linear features are a natural way of summarizing important structure. For instance in the brain, a large subset of the crest lines correspond to gyri and sulci and in Subsol et al [37] these features were extracted from different brains and registered to a reference to construct a crest-line atlas. Such atlases succinctly summarize population anatomical variation. As point and line matching is relatively fast to compute, a large number of solutions and potential correspondences can be explored. Other related applications include the registration of vascular images where the structures of interest are "tubes" [38, 39]. Many non-rigid registration methods based on 3D geometric features use anatomical surfaces, for example the shape of the left ventricle [40]. Typically, surface-based registration algorithms can be decomposed into three components: extracting boundary points of interesting structures in the image, matching the source and reference surface, and then extending the surface-based transformation to the full volume. There are many different ways to implement each of these steps. For example, Thompson et al extract the surfaces of the lateral ventricle and the cerebral cortex in a subject's brain scan and in a corresponding brain atlas automatically [41]. In Audette et al [42] brain and skin surfaces in pre-operative MR and CT images and intraoperative range images are extracted using the powerful level-set framework [43] and registered to track intraoperative brain deformation. Other authors have used elastic [44] and boundary mapping [45] techniques. The related task of tracking MR brain deformation in intraoperative images is achieved in Ferrant et al [46] by registering cortical and ventricle surfaces and using a biomechanical model of brain tissue to infer volumetric brain deformation. A detailed survey of surface-based medical image registration can be found in Audette et al [47].

Intensity approaches match intensity patterns in each image using mathematical or statistical criteria. They define a measure of intensity similarity between the source and the target and adjust the transformation until the similarity measure is maximized. They assume that the images will be most similar at the correct registration. Measures of similarity have included squared differences in intensities, correlation coefficient, measures based on optical flow, and information-theoretic measures such as mutual information. The simplest similarity measure is the sum of squared differences, which assumes that the images are identical at registration except for (Gaussian) noise. The correlation coefficient assumes that corresponding intensities in the images have a linear relationship. These two similarity measures are suitable for mono-modal registration where the intensity characteristics are very similar in the images. For multi-modal registration, similarity measures have been developed, which define weaker relationships between intensities to reflect the different intensity characteristics of different imaging modalities. The correlation ratio [48] assumes that corresponding intensities are functionally related at registration and information-theoretic measures like mutual information assume only that a probabilistic relationship between voxel intensities is maximized at registration. All these measures are discussed at greater length in Hajnal et al [10] and defined more precisely in Table 1.

Intensity-based registrations match intensity patterns over the whole image but do not use anatomical knowledge. Geometric registration uses anatomical information but usually sparsely distributed throughout the images. Combining geometric features and intensity features in registration should result in more robust methods. Hybrid algorithms are therefore of particular current interest, combining intensity-based and model-based criteria to establish more accurate correspondences in difficult registration problems, *e.g.* using sulcal information to constrain intensity-based brain registration [49, 50] or to combine the cortical surface with a volumetric approach [51]. Surfaces are also used to drive volumetric registration in Thompson et al [52] to analyse normal and Alzheimer brains with respect to an anatomical image database. In Christensen et al [53] the registration task is to correct for large displacement and deformation of pelvic organs induced when intracavity CT applicators are used to treat advanced cancer of the cervix. Anatomical landmarks are used to initialize an intensity driven fluid registration with both stages using the same model for tissue deformation. In this application the more robust but less flexible landmark registration produces a robust starting position for the less robust but more flexible fluid registration and the two steps run serially (there is further discussion of fluid registration in the next section). Other researchers have attempted true hybrid solutions where intensity and feature information are incorporated into a single similarity measure, *e.g.* in Russakoff et al [54] a rigid registration is computed between a pre-operative spinal CT and an intraoperative X-ray by maximizing the difference of a mutual information based intensity measure and a distance between corresponding landmarks. As is often the case, an additional parameter has to be chosen empirically to appropriately weight the intensity and landmark parts of the similarity measure. A more sophisticated approach built on the same principles is used in PASHA (Pair And Smooth Hybrid Algorithm) [55] where the similarity measure is the weighted sum of an intensity similarity, a term expressing the difference between the landmark correspondence and the volumetric deformation field, and a smoothing term. In Hellier and Barillot [50] a framework for incorporating landmark constraints with image-based non-rigid registration is

Table 1. Common image similarity measures used in registration. Here $T(\mathrm{x})$ is the intensity at a position x in an image and $S(t(\mathrm{x}))$ is the intensity at the corresponding point given by the current estimate of the transformation $t(\mathrm{x})$. N is the number of voxels in the region of overlap

Voxel similarity measure	Comment
Sum of Squared Differences $\text{SSD} = \frac{1}{N} \sum_{\mathrm{X}} \left(T(\mathbf{x}) - S(t(\mathbf{x})) \right)^2$	Registered images differ only by Gaussian noise. Sensitive to small number of voxels that have very large intensity differences. Only for mono-modal image registration
Correlation coefficient $CC = \dfrac{\sum_{\mathrm{x}} (T(\mathbf{x}) - \bar{T}) \cdot \left(S(t(\mathbf{x})) - \bar{S} \right)}{\sqrt{\sum_{\mathrm{x}} (T(\mathbf{x}) - \bar{T})^2 \cdot \sum_{\mathrm{x}} \left(S(t(\mathbf{x})) - \bar{S} \right)^2}}$	Registered images have linear intensity relationship and objects of interest are in the field of view of both images. Segmentation of interesting features often necessary. Only for single-modal image registration
Correlation ratio $\eta = 1 - \frac{1}{N\sigma^2} \sum_{i} N_i \sigma_i^2$	The correlation ratio assumes a functional relationship between intensities. It can be defined in terms of sums and sums of squares of source voxels that correspond to a number N_i of iso-intense voxels in the target image $\sigma^2 = \dfrac{1}{N} \sum_{\text{overlap x}} S(\mathbf{x})^2 - m^2, m = \dfrac{1}{N} \sum_{\text{overlap x}} S(\mathbf{x})$ $\sigma_{\mathrm{i}}^2 = \dfrac{1}{N_i} \sum_{\mathbf{x}: T(\mathbf{x}) = i} S(\mathbf{x})^2 - m_i^2, m_i = \dfrac{1}{N_i} \sum_{\mathbf{x}: T(\mathbf{x}) = i} S(\mathbf{x})$
Mutual information $\text{MI} = H_T + H_S - H_{TS}$	Assumes only a probabilistic relationship between intensities. Defined in terms of entropies of the intensity distribution $H_T = -\sum_i P_i \log P_i, H_S = -\sum_j Q_j \log Q_j$ and $H_{TS} = -\sum_{i,j} p_{ij} \log p_{ij}$ where P (Q) = probability of intensity I (J) occurring in target (source) and p_{ij} = joint probability of both occurring at the same place
Normalized mutual information $\text{NMI} = \frac{H_T + H_S}{H_{TS}}$	Proposed to minimize the overlap problem seen occasionally with mutual information

described for the application of intersubject brain registration where the constraints ensure that homologous sulci are well matched.

Transformation models

The transformation model defines how one image can be deformed to match another; it characterizes the type and number of possible deformations. The most well known example is the rigid or affine transformation that can be described very compactly by between 6 (3 translations and 3 rotations) and 12 (6 + 3 scalings + 3 shears) parameters for a whole image. These parameters are applied to a vector locating a point in an image to find its location in another image. The transformation model serves two purposes; first it controls how image features can be moved relative to one another to improve the image similarity and second it interpolates between those features where there is no useable information. Transformations used in non-rigid registration range from smooth regional variation described by a small number of parameters [56] to dense displacement fields defined at each voxel [2]. One of the most important transformations is the family of splines that have been used in various forms for around 15 years. Spline-based registration algorithms use corresponding ("control") points, in the source and target image and a spline function to define correspondences away from these points. The "thin-plate" spline [57] has been used extensively to investigate subtle morphometric variation in schizophrenia [58–60]. Each control point belonging to a thin-plate spline has a global influence on the transformation in that, if its position is perturbed, all other points in the transformed image change. This can be a disadvantage because it limits the ability to model complex and localized

deformations and because, as the number of control points increases, the computational cost associated with moving a single point rises steeply. By contrast, B-splines are only defined in the vicinity of each control point; perturbing the position of one control point only affects the transformation in the neighbourhood of the point. Because of this property, B-splines are often referred to as having "local support". B-spline based non-rigid registration techniques [25] are popular due to their general applicability, transparency and computational efficiency. Their main disadvantage is that special measures are sometimes required to prevent folding of the deformation field and these measures become more difficult to enforce at finer resolutions. Such problems have not prevented these techniques finding widespread use (in the brain [61], the chest [62] the heart [63, 64], the liver [65], the breast [66, 67] etc.). Elastic models treat the source image as a linear, elastic solid [68] and deform it using forces derived from an image similarity measure. The elastic model results in an internal force that opposes the external image matching force. The image is deformed until the forces reach equilibrium. Since the linear elasticity assumption is only valid for small deformations it is hard to recover large image differences with these techniques. Replacing the elastic model by a viscous fluid model [69] allows large and highly localized deformations. The higher flexibility increases the opportunity for misregistration, generally involving the growth of one region instead of a shifting or distorting another [16]. According to BroNielsen and Gramkow [70] another non-rigid technique, the "demons" algorithm [71, 72], can be thought of as an approximation to fluid registration. Finite element (FE) models allow more principled control of localized deformations and have been applied particularly to the head for surgical

scenarios [12, 73]. These models divide the image into cells and assign to these cells a local physical description of the anatomical structure. For instance, soft tissue can be labelled as elastic, bone as rigid and cerebrospinal fluid (CSF) as fluid. External forces such as landmark correspondences or voxel similarity measures are applied to the model, which deforms according to the material behaviour in each cell. Such approaches tend to be used where there are strong biomechanical constraints in operation, *i.e.* they are appropriate for serial registration of images of brains undergoing some mechanical intervention but not appropriate for intersubject registration. Where registration speed is important some researchers have applied optical flow techniques that were originally developed in the computer vision and artificial intelligence community. Some adaptation has been required for medical applications because the "constant intensity" assumption is often (usually!) broken in serial medical images and optical flow methods have not been widely adopted. Nevertheless optical flow based registration has enjoyed some success in tracking myocardial tags [74], aligning CT lung images [75], registering breast images [76] and registering real and virtual endoscopic images [77].

Optimization

Optimization refers to the manner in which the transformation is adjusted to improve the image similarity. A good optimizer is one that reliably and quickly finds the best possible transformation. Choosing a good optimizer requires a good understanding of the registration problem, the constraints that can be applied and knowledge of numerical analysis. An in depth discussion of optimization is far beyond the scope of this paper. In non-rigid registration applications choosing or designing an optimizer can be difficult because the more non-rigid (or flexible) the transformation model the more parameters are generally required to describe it. For the optimizer this means that more time is required to make a parameter choice and that there is more chance of choosing a set of parameters, which result in a good image match which is nevertheless not the best one (the "local minima" problem). A more subtle problem is that a transformation parameter choice that gives a good image or feature similarity may not be physically meaningful. The most common example of this is when we have a prior belief that the registration of one image onto another should be diffeomorphic; in simple terms this means that if the transformation were applied to a real physical object to deform it then no tearing of the object would occur. The problem is that tearing can often result in a transformation that makes the images more similar despite it being physically invalid. Therefore in many situations, *e.g.* serial MR brain registration of a subject undergoing diffuse atrophy, there is a prior expectation that folding or tearing should not be required to secure a good match. One of the attractions of fluid registration [69] that has been successfully used in this application [2, 78] is that the transformation model implicitly forbids tearing. Often, tearing is a result of correspondence problems. For instance, intersubject brain registration where one subject has a large extrinsic tumour and abdominal registration where fluid and gas filled spaces can appear and disappear

between scans are examples where correspondence is not well defined and where tearing or folding may be necessary to describe the underlying physical transformation. Other constraints can be implicit in the choice of the transformation model, *e.g.* that the transformation should be consistent with the behaviour of a deforming elastic body. Much of the work of optimizers is therefore to balance the competing demands of finding the best set of correspondences subject to application-specific constraints.

The most common optimizer for registering point sets is the Iterative Closest Point algorithm of Besl and McKay [79], which does not require all the pair-wise correspondences of landmarks to be pre-defined and which iterates towards the nearest local error minimum. Some more recent algorithms solve a similar problem with similar performance and some claimed advantages in robustness to local minima [80] and convergence properties [81]. Many registration algorithms are amenable to existing optimization schemes in that they seek to choose a set of parameters to maximize (or minimize) a function. This is a standard problem and there are standard ways to solve it (*e.g.* Downhill Simplex Method, Powell's Method, Steepest Gradient Descent, the Conjugate Gradient Method etc. [82]). Fluid and elastic transformations that can be described in terms of a partial differential equation (PDE) can be obtained using existing numerical solvers (successive over relaxation, full multi-grid etc. [2, 69, 82]). Which optimization scheme is suitable for a particular registration application depends on the cost function, the transformation, potential time-constraints, and the required accuracy of the registration.

Validation

Validation usually means showing that a registration algorithm applied to typical data in a given application consistently succeeds with a maximum (or average) error acceptable for the application. For geometric approaches a real-world error can be computed, which for landmark methods expresses the distance between corresponding landmarks post-registration. For rigid-registration this form of error analysis has been studied intensively and it has been found that an average target registration error for the whole volume can be estimated from knowledge of the landmark positions [83]. Such an analysis is not generally possible for non-rigid techniques so although the error at landmarks can be established, the error in other parts of the volume is dependent on the transformation model and must be estimated using other means. In intensity-based approaches the registration itself, usually cannot inform the user of success or failure, as the image similarity measure is not related to real-world error in a simple way. For these problems, validation is usually performed by making additional measurements post-registration or showing that an algorithm performs as desired on pairs of test images for which the transformation is known. One common approach is to identify corresponding landmarks or regions independently of the registration process and establish how well the registration brings them into alignment [56, 84]. In Schnabel et al [66] a biomechanical model of the human breast is used to simulate MR images of a breast subject to mechanical forces as might be experienced during biopsy or movement

during dynamic contrast-enhanced imaging. Pre- and post-contrast images subject to known deformation were generated and used to validate a B-spline based non-rigid registration. Of course in many applications the true point-to-point correspondence can never be known and may not even exist (*e.g.* intersubject brain registration). Various kinds of consistency test are also used in validation; the most common are establishing that registration of source to target produces the same alignment as from target to source (this is commonly not the case for non-rigid registration) or that for three images, A, B, C, registration of C→A gives the same result as C→B compounded with B→A [85]. It is important to carefully pose the registration task in application specific terms that make use of available information in the image and prior knowledge. These issues are discussed in some depth for brain registration problems in Crum et al [27]. In most applications, careful visual inspection remains the first and most important validation check available for previously unseen data.

Applications

Rigid registration is well established as a research tool, and is becoming widely available in clinical products (such as on workstations provided by scanner vendors). Non-rigid registration is only gradually being adopted, partly due to the difficulties in validation described above. Nevertheless there is a growing body of published work that focuses on real-world applications of non-rigid registration rather than technical refinements. In this section we briefly review this work and suggest areas where the use of non-rigid registration is likely to increase in importance.

Non-rigid registration is a key requirement for the application of biomechanical models of cardiac function. A recent methodology involves the creation of a generic cardiac model that is instantiated by linear elastic registration with cardiac images of a subject acquired with more than one imaging modality [86]. Each image allows different mechanical parameters (*e.g.* muscle fibre direction from diffusion tensor imaging, regional tissue segmentation from MRI etc.) to be assigned to the model increasing its validity as a representation of the cardiac function of the individual. The model has been used to track heart motion in time-series of SPECT and MRI images and estimate the ejection fraction. In other work, a two-stage non-rigid registration approach is used to enable direct comparison of cardiac motion fields between individuals imaged using tagged MRI [87]. Each tagged frame was registered back to the end-diastolic frame using B-spline registration. Then untagged end-diastolic frames were registered between individuals allowing direct comparison of cardiac motion in a single reference frame. This work is still at a relatively early stage but has huge potential. The use of gated myocardial perfusion SPECT to assess left ventricular function and perfusion can be improved by using registration to remove left ventricular motion to allow perfusion image to be visualized in a static coordinate system. Slomka et al [88] attempt this by sampling the epicardial and endocardial surfaces and matching all phases to the end-diastolic phase using thin-plate splines. They argue that the effective resolution of the technique is improved by removing motion-related blur

which should lead to improvements in the ability to detect coronary artery disease. Respiratory motion remains a problem in cardiac imaging. Strategies such as breath-hold and navigator-gated imaging have been employed to reduce the effects of breathing motion but are not universally successful. McLeish et al [64] used non-rigid registration to study the motion of the heart during the breathing cycle. For images acquired at the same cardiac phase at different stages of inhalation significant deformation (∼3–4 mm) was observed in the free wall of the right atrium and the left ventricle.

There is growing interest in applying registration to other organs subject to motion and non-rigid deformation often with a view to tracking their position and shape during breathing to allow delivery of targeted treatments for cancer such as external beam radiotherapy or thermal/cryo ablation. This often involves registration of planning images acquired pre-treatment, possibly on a different day at a different site, with images acquired during treatment. For some organs there will be gross deformations owing to patient positioning as well as differences owing to different stomach, bowel and bladder contents, and owing to breathing. Several authors have used registration to quantify the motion and deformation of the liver during breathing as a precursor to tracking motion. Rohlfing et al [65] used breathing gated acquisitions to acquire MR liver images in normal subjects and then applied rigid followed by non-rigid registration to match each breathing phase with the end-expiration image. They found that non-rigid deformation varied between 1 cm and 3 cm in the liver across all subjects. Blackall et al [89] adopted a more sophisticated approach to the motion analysis in an earlier study by constructing a statistical model and extracting principal components of motion and deformation. They found typical deformation magnitudes of between 1 cm and 1.5 cm with the superior and inferior surfaces of the liver experiencing the most deformation.

The motion of lungs during the breathing cycle is also of interest, especially for external beam radiotherapy applications. Gee et al [90] use elastic registration to track lung motion in MR images acquired during normal breathing and to quantify the deformation, calculate local strains from the registration displacement field. Boldea et al [91] use the Demons registration algorithm to detect lung deformation in CT scans of images acquired while the subjects used an active breath control device to stop inhalation or expiration at a specified lung volume. The technique verified that breath-holding was effective and in one case, detected a partial lung collapse that occurred between acquisitions. Another application where breathing must be accommodated is using CT chest images (acquired in a maximum inspiration 30 s breath-hold) to provide high resolution anatomical context to PET functional scans (acquired over 30 min with free breathing) [62]. The PET image is an average over the breathing cycle whereas the CT scan is a snapshot during the breathing cycle. Using a careful visual assessment of 27 subjects the authors established that the largest registration errors occurred in the abdomen (mean ∼1.5–2.5 PET voxel dimensions) and the smallest errors occurred in the mid to upper lung regions (mean ∼0–1.5 PET voxel dimensions). To standardize anatomy between subjects, Li et al [3] used a combination of rigid and non-rigid inverse-consistent

registration techniques to align CT lung volumes from six individuals. The registration was constrained using 10–15 airway branch points manually identified in each lung. Dougherty et al [75] used optical flow to register lung volumes acquired from the same individual at different times to enable serial analysis of lung structure. The
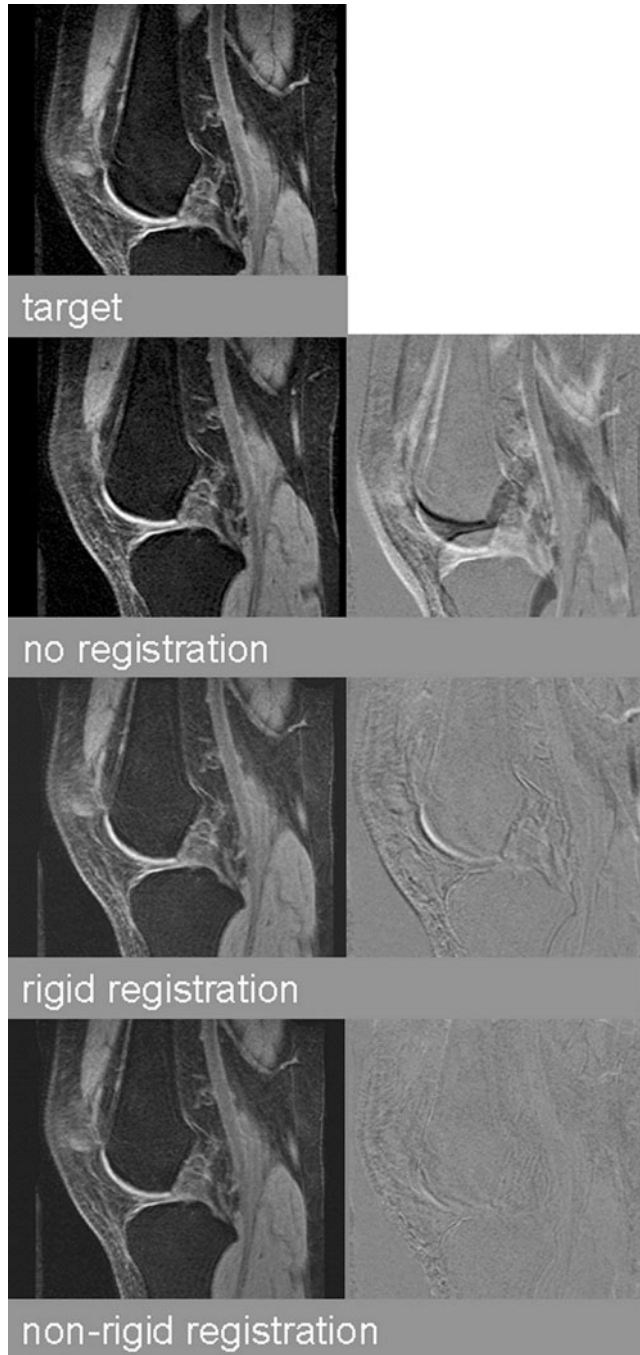

Figure 2. A more unusual application is registering images of knee joints for the purpose of tracking changes in the thickness of cartilage. The knee is particularly difficult to image consistently in three dimensions on consecutive occasions due to the high degree of mobility around the joint regardless of any disease process. Non-rigid registration, in this case using B-spline based free-form deformations, can recover most of the differences between scans of the same subject acquired at different times.

method did not require any manual delineation of landmarks but did not have to accommodate inter-individual differences in anatomy either.

Central to the use of registration in radiotherapy is its use to calculate localized dose distributions, which in common with precise delivery techniques has the potential to allow higher doses to be delivered to cancerous tissue without harming nearby normal tissue. Several groups have applied non-rigid registration to align the prostate and surrounding structures with this in mind. Fei et al [92] compared rigid (volumetric) and thin-plate spline (iterated control-point) registration of MR pelvic volumes to correct for (a) diagnosis versus treatment positioning; (b) full-bladder versus empty bladder with repositioning; (c) diagnosis versus diagnosis positioning with a week between scans; and (d) diagnosis versus diagnosis with repositioning. They found that non-rigid registration was necessary to achieve a good match when repositioning was significant but that >120 control points were required in the pelvic volume to achieve a good result (defined as sub-millimetre residual error in the centroid of the prostate). A biomechanical model of the prostate has also been used to
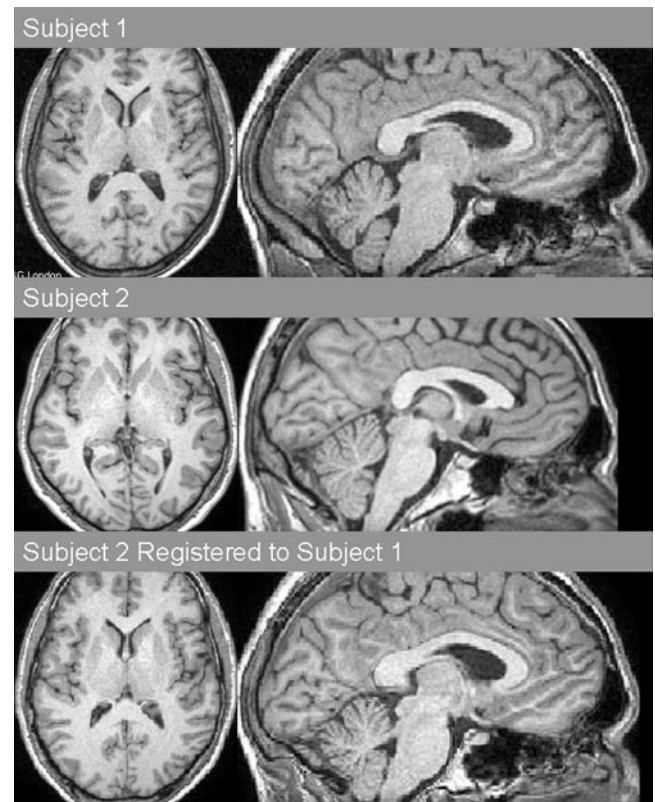

Figure 3. Non-rigid registration applied to intersubject brain matching. The top row shows two selected slices from a T_1 weighted MR-volume of a normal subject. The middle row shows the same slices from a similar image of a different subject. The bottom row shows the result of using non-rigid (fluid) registration to match the second subject to the first. The major neuroanatomical features have been brought into good correspondence. A closer inspection shows that not all of the fine cortical structure has been matched successfully. This is a typical finding when comparing brain images across subjects due to population variation in the geometry of the cortical surface. Note, the left and right views are not of the same scale.

correct for differences in positioning and scanning protocol between pre-operative 1.5 T MR images and 0.5 T MR images acquired during brachytherapy sessions [93]. Schaly et al [94] used thin-plate-spline registration to show that significant differences in rectum, bladder and seminal vesicle doses compared with the planned dose are possible due to motion both within fractions and between daily fractions.

Another area where patient positioning and reproducible imaging is very difficult is in imaging of joints. Work in is this area is at a relatively early stage but there are already some obvious applications such as to track changes in the thickness of cartilage plates over time [95]. In Figure 2 the ability of non-rigid registration based on B-splines to correct for repositioning problems in MR images of a volunteer is shown. There are many potential applications in the study and monitoring of diseases such as osteoarthritis.

At the time of writing, it is only in brain applications that non-rigid registration is used on a routine basis even though there remain some questions about its veracity [27, 96–98]. Perhaps the most common application is so-called "spatial normalization" [5, 99], where it is desired to place a number of brain images into a single reference frame for detailed structural or functional comparison (Figure 3). The SPM package provides a means to do this using a standard template brain and a non-rigid registration based on discrete cosine basis functions. A large number of structural MR brain studies have been performed using this framework investigating ageing [100], dementia [101–105], epilepsy [106, 107], schizophrenia [108, 109] etc. It is well known that normalizing to a specific template can introduce bias either by registering to a particular brain that has its own structural peculiarities and/or by forcing a pre-ordained anatomical coordinate system on each brain in a study. One solution to this is to register all brains to a reference frame that minimizes the total "distance" between itself and each brain and this is an area of current research [110, 111]. Non-rigid registration algorithms are computationally demanding, which makes analysis techniques using registration slow, especially when images of large numbers of subjects are involved. Recent work has shown how innovations in internet technology such as computational grids can couple image analysis algorithms, databases and distributed computing to provide high-throughput image analysis. A recent application used grid technology to database a large number of labelled MR brain images registered to a standard template. A dynamic atlas could then be constructed on demand, using the grid for speed, and matching user preferences such as age, sex, disease, disease-stage etc. [112]. Such dynamic atlases can be
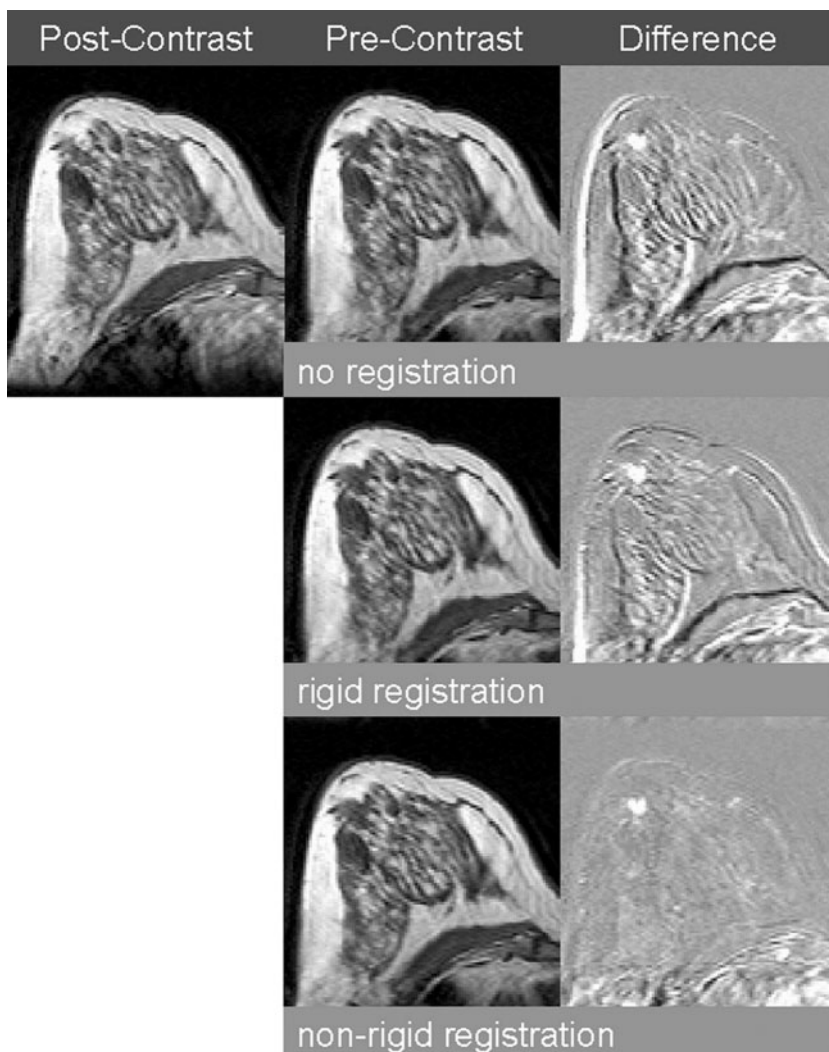

Figure 4. Non-rigid registration applied to lesion detection in contrast-enhanced MR mammography. The subject is scanned at rest and then scanned repeatedly after introduction of a contrast agent. There is often rigid and non-rigid movement when the agent is given. The pre- and post-contrast images appear virtually identical but subtraction reveals many differences (top panel), most caused by motion. Rigid registration (middle panel) reduces the difference between scans significantly. Non-rigid registration using a hierarchical B-spline technique (bottom panel) removes virtually all the artefact associated with motion leaving clear evidence of an enhancing lesion.

used to label a new brain image or to classify it into a disease category. Disease-specific atlases carefully constructed using elastic registration of cortical surfaces and major sulci had also previously been used to analyse structural changes in early Alzheimer's disease [13]. Another area where image registration coupled with large computer resources is likely to be applied is in large-scale animal (and ultimately human) morphological studies for genomic and phenomic investigation and drug discovery [113].

In contrast to the group-based studies above, another brain application of non-rigid registration is in monitoring change in the individual by acquiring serial scans. This has been particularly useful in dementia where fluid registration has proven useful for visualizing patterns of regional atrophy [2, 78]. Studies have also been carried out in multiple sclerosis to improve the power of analytical techniques by using non-rigid registration as part of a pipeline to transform serial scans into a four-dimensional space for spatiotemporal analysis [114, 115]. Non-rigid registration has also been used to quantify surgical brain shift by registering post-operative and intraoperative MR images with pre-operative images using free-form deformations [116] and linear elastic finite element models driven by surface deformation [46].

The increasing use of contrast-enhanced MRI breast imaging has generated problems, which can be solved by registration (Figure 4). Early work by Davis et al [117] and Rueckert et al [25] used elastic-body splines and B-splines, respectively, to correct for motion before and after contrast injection and between scans acquired over time, *e.g.* to track response to chemotherapy. This problem has also been studied by Bruckner et al [118] where rigid registration was compared with an elastic non-rigid registration algorithm. These studies utilized common structural information in the images to be registered but did not deal explicitly with the presence or absence of contrast agent. In Hayton et al [76] a careful consideration of possible patient motions during dynamic MR image acquisition is combined with a simple model for contrast uptake in a 2D registration algorithm based on optical flow. Where a physical process is affecting image contrast in a series of images, modelling the effect of that process on the appearance of image structure is a powerful approach. In Rohlfing et al [119] and Tanner et al [67] volume-preserving constraints are applied during registration of dynamic images to reduce the effect of enhancing regions on the intensity based registration. Non-rigid registration has also been used to correct for varying amounts of breast deformation in 3D free-hand ultrasound acquisition [120].

A generic application of non-rigid registration is in segmentation or labelling. The general idea is that an image exists with structures or tissue classes labelled already and it is desired to label a new image. If non-rigid registration can achieve a good correspondence between structurally equivalent regions on the two images then the labels can be transferred from one image to another and the problem is solved. Brain segmentation has been explored using this technique [84, 121–123]. The amount of deformation that each label undergoes when being matched to the target brain can also be used for volumetric [61, 124] or morphometric analysis. An ambitious attempt to construct a CT atlas of the liver,

kidneys and spinal cord is described in Park et al [125] where thin-plate splines and mutual information were used to register 31 CT images to a reference. The resulting tissue probability maps were then applied to organ segmentation in 20 further scans. In Noble et al [126] non-rigid registration was used to propagate manual delineation of epicardial and endocardial boundaries on a single slice first to other slices in the volume and then to other cardiac phases in an acquisition. Epicardial volumes computed from the automated method compared favourably with manual delineations. An example of this process is shown in Figure 5.
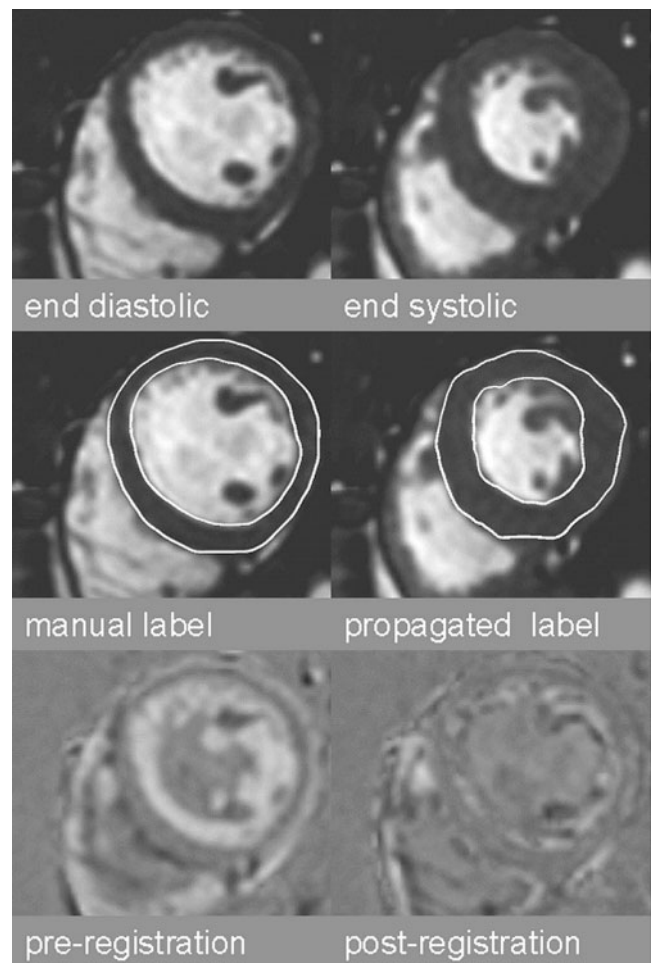

Figure 5. Non-rigid registration applied to myocardial segmentation. In this example the myocardium has been manually delineated on each slice of the end-diastolic phase to define a surface. The end-diastolic image volume has been registered to the end-systolic volume to delineate the myocardium at end systole. Technical details: the images are short axis electrocardiogram triggered SSFP SENSE factor 2 images from a healthy volunteer collected on a Philips Intera 1.5 T scanner (Philips Medical Systems, Best, The Netherlands) at Guy's Hospital, London, UK. 20 cardiac phases were acquired with each volume consisting of 12–14 contiguous slices, collected in blocks of three, during up to five breath-holds. Registration was performed with vtknreg (available free from www.image-registration.com), which uses free-form deformations modelled with B-splines.
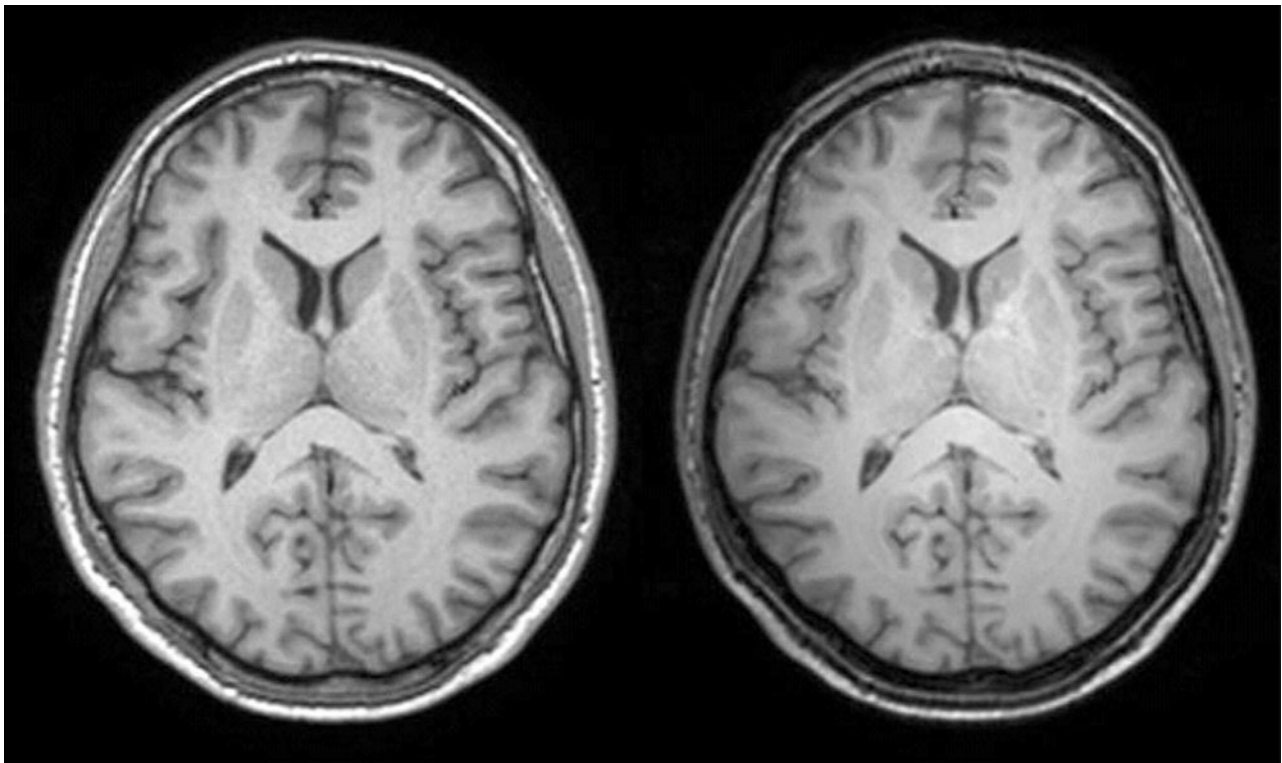
Figure 6. An example of 1.5 T versus 3 T MRI of the brain. It must be remembered that image acquisition is evolving along with image registration. With new imaging opportunities come new registration challenges. This pair of corresponding slices from rigidly registered brains acquired on two different scanners have exactly the same structure but appear subtly different, despite efforts to match the image acquisition schemes. The 3 T image has higher signal to noise ratio than the 1.5 T image but is also more prone to image artefacts, most obviously here in significant amounts of signal inhomogeneity across the brain (so-called "shading artefact"), and also flow artefacts from the carotid arteries. Registration algorithms driven by intensity information find it hard to differentiate between image differences caused by biological processes and those caused by details of the acquisition process. Image analysis studies that migrate from 1.5 T to 3 T scanners, or which involve aggregation of scans collected from scanners of different field strength are likely to have problems separating real effects from scanner-induced effects.

Conclusions

Image registration is becoming a core technology for many imaging tasks. For example, reliable analysis of functional images such as BOLD MRI and perfusion MRI is not possible without image registration to compensate for subject motion during scanning. For functional brain studies, rigid registration is sufficient, but for most other parts of the body, non-rigid registration is required. Non-rigid registration of a subject image to a reference image is also increasingly being used as a way of automatically segmenting structures of interest from scans. Furthermore, registration is being used not just as part of the post-processing of images, but also in the acquisition and reconstruction of images. These trends mean that image registration – especially rigid registration – will soon be widely used clinically without the user even being aware it is happening. The two obstacles to widespread clinical use of non-rigid registration are the computational cost and the difficulty in validating the results. The most sophisticated non-rigid registration algorithms frequently take many hours to register images, which makes them unsuitable for interactive use on image analysis work-stations or on scanner consoles. For non-rigid registration to become widely used clinically, there will either need to be huge improvements in algorithm performance, or a willingness to allow the analysis to be run "off-line",

just as tomographic image reconstruction once was. For clinical users to be prepared to wait for the registration results, the difficulties in validation discussed earlier will need to be addressed. Another important point is that the field of imaging is advancing in parallel with the field of image analysis. Figure 6 shows the changing nature of MRI as more centres have access to improved imaging technology. In this case the improvement in image quality moving from 1.5 T acquisition to 3 T acquisition is apparent but so are the increased problems of image artefacts. Registration solutions constructed for particular types of images do not always perform as well when the imaging conditions change. This field is moving rapidly and provided that confidence in registration technology can be maintained at a high level, non-rigid registration is likely to become an increasingly important component of 21st century medical imaging systems.

Acknowledgments

GlaxoSmithKline, (Figure 2), B Sneller, funded by EPSRC, (Figures 3, 6), C Tanner, funded by EPSRC, (Figure 4), and Dr N Noble, funded by Philips Medical Systems Nederland B.V. Medical Imaging Information Technology – Advanced Development (Figure 5). Jo Hajnal of Imperial College supplied the 3T image in Figure 6. The authors acknowledge that many research groups around the world could have provided similar high-quality examples of non-rigid registration for this article.

References

1. Hill DLG, Batchelor PG, Holden M, Hawkes DJ. Medical image registration. Phys Med Biol 2001;46:R1–R45.
2. Freeborough PA, Fox NC. Modeling brain deformations in Alzheimer disease by fluid registration of serial 3D MR images. J Comput Assist Tomogr 1998;22:838–43.
3. Li BJ, Christensen GE, Hoffman EA, McLennan G, Reinhardt JM. Establishing a normative atlas of the human lung: intersubject warping and registration of volumetric CT images. Acad Radiol 2003;10:255–65.
4. Orchard J, Greif C, Golub GH, Bjornson B, Atkins MS. Simultaneous registration and activation detection for fMRI. IEEE Trans Med Imaging 2003;22:1427–35.
5. Ashburner J, Friston KJ. Nonlinear spatial normalization using basis functions. Human Brain Mapping 1999;7:254–66.
6. Bidaut LM, Vallee JP. Automated registration of dynamic MR images for the quantification of myocardial perfusion. J Magn Reson Imaging 2001;13:648–55.
7. McLeish K, Kozerke S, Crum WR, Hill DLG. Free breathing radial acquisitions of the heart. Magn Reson Med 2004;52:1127–35.
8. Pelizzari CA, Chen GTY, Spelbring DR, Weichselbaum RR, Chen CT. Accurate 3-dimensional registration of CT, PET, and/or MR images of the brain. J Comput Assist Tomogr 1989;13:20–6.
9. Hill DLG, Hawkes DJ, Crossman JE, Gleeson MJ, Cox TCS, Bracey EECML, et al. Registration of MR and CT images for skull base surgery using point-like anatomical features. Br J Radiol 1991;64:1030–5.
10. Hajnal JV, Hill DLG, Hawkes DJ, editors. In: Medical image registration. CRC Press Boca Raton, 2001.
11. Hawkes DJ, Barratt D, Blackall JM, Chan C, Edwards PJ, Rhode K, et al. Tissue deformation and shape models in image-guided interventions: a discussion paper. Med Image Anal 2004; In Press.
12. Ferrant M, Nabavi A, Macq B, Black PM, Jolesz FA, Kikinis R, et al. Serial registration of intraoperative MR images of the brain. Med Image Anal 2002;6:337–59.
13. Thompson PM, Mega MS, Woods RP, Zoumalan CI, Lindshield CJ, Blanton RE, et al. Cortical change in Alzheimer's disease detected with a disease-specific population-based brain atlas. Cerebral Cortex 2001;11:1–16.
14. Thompson PM, Giedd JN, Woods RP, MacDonald D, Evans AC, Toga AW. Growth patterns in the developing human brain detected using continuum-mechanical tensor mapping. Nature 2000;404:190–3.
15. Brown LG. A survey of image registration techniques. Computing Surveys 1992;24:325–76.
16. Lester H, Arridge SR. A survey of hierarchical non-linear medical image registration. Pattern Recognition 1999;32:129–49.
17. Maintz JBA, Viergever MA. A survey of medical image registration. Med Image Anal 1998;2:1–36.
18. Zitova B, Flusser J. Image registration methods: a survey. Image Vision Comput 2003;21:977–1000.
19. Makela T, Clarysse P, Sipila O, Pauna N, Pham QC, Katila T, et al. A review of cardiac image registration methods. IEEE Trans Med Imaging 2002;21:1011–21.
20. Hutton BF, Braun M, Thurfjell L, Lau DYH. Image registration: an essential tool for nuclear medicine. Eur J Nucl Med Mol Imaging 2002;29:559–77.
21. Rosenman JG, Miller EP, Tracton G, Cullip TJ. Image registration: an essential part of radiation therapy treatment planning. Int J Radiat Oncol Biol Phys 1998;40:197–205.
22. Meijering EHW, Niessen WJ, Viergever MA. Retrospective motion correction in digital subtraction angiography: a review. IEEE Trans Med Imaging 1999;18:2–21.
23. Toga AW, Thompson PM. The role of image registration in brain mapping. Image Vision Comput 2001;19:3–24 Sp. Iss.
24. Thompson PM, Woods RP, Mega MS, Toga AW. Mathematical/computational challenges in creating deformable and probabilistic atlases of the human brain. Human Brain Mapping 2000;9:81–92.
25. Rueckert D, Sonoda LI, Hayes C, Hill DLG, Leach MO, Hawkes DJ. Nonrigid registration using free-form deformations: application to breast MR images. IEEE Trans Med Imaging 1999;18:712–21.
26. Johnson HJ, Christensen GE. Consistent landmark and intensity-based image registration. IEEE Trans Med Imaging 2002;21:450–61.
27. Crum WR, Griffin LD, Hill DLG, Hawkes DJ. Zen and the art of medical image registration: correspondence, homology, and quality. NeuroImage 2003;20:1425–37.
28. Rohr K. Landmark-based image analysis: using geometric and intensity models. Volume 21 of Computational Imaging and Vision Series. Dordrecht, Boston, London: Kluwer Academic Publishers, 2001.
29. Rohr K, Stiehl HS, Sprengel R, Beil W, Buzug TM, Weese J, et al. Point-based elastic registration of medical image data using approximating thin-plate splines. Visualization in Biomedical Computing, Lecture Notes in Computer Science 1996;1131:297–306.
30. Thirion JP, Gourdon A. Computing the differential characteristics of isointensity surfaces. Comput Vision Image Understanding 1995;61:190–202.
31. Beil W, Rohr K, Stiehl HS. Investigation of approaches for the localization of anatomical landmarks in 3D medical images. In: H Lemke, M Vannier, K Inamura, editors. Proc Computer Assisted Radiology and Surgery. Berlin, Germany: Elsevier Science, 1997: 265–70.
32. Rohr K, Stiehl HS, Sprengel R, Buzug TM, Weese J, Kuhn MH. Landmark-based elastic registration using approximating thin-plate splines. IEEE Trans Med Imaging 2001;20:526–34.
33. Rohr K, Fornefett M, Stiehl HS. Spline-based elastic image registration: integration of landmark errors and orientation attributes. Comput Vision Image Understanding 2003;90:153–68.
34. Monga O, Benayoun S. Using partial derivatives of 3D images to extract typical surface features. Comput Vision Image Understanding 1995;61:171–89.
35. Maintz JBA, vandenElsen PA, Viergever MA. Evaluation of ridge seeking operators for multimodality medical image matching. IEEE Trans Pattern Anal 1996;18:353–65.
36. Lindeberg T. Edge detection and ridge detection with automatic scale selection. Int J Comput Vision 1998;30:117–54.
37. Subsol G, Roberts N, Doran M, Thirion JP, Whitehouse GH. Automatic analysis of cerebral atrophy. Magn Reson Imaging 1997;15:917–27.
38. Aylward SR, Jomier J, Weeks S, Bullitt E. Registration and analysis of vascular images. Int J Comput Vision 2003;55:123–38.

39. Aylward SR, Bullitt E. Initialization, noise, singularities, and scale in height ridge traversal for tubular object centerline extraction. IEEE Trans Med Imaging 2002;21:61–75.

40. Chen CW, Huang TS, Arrott M. Modeling, analysis and visualization of left ventricle shape and motion by hierarchical decomposition. IEEE Trans Pattern Anal Machine Intelligence 1994;16:342–56.

41. Thompson PM, Toga AW. A surface-based technique for warping three-dimensional images of the brain. IEEE Trans Med Imaging 1996;15:402–17.

42. Audette MA, Siddiqi K, Peters TM. Level-set surface segmentation and fast cortical range image tracking for computing intrasurgical deformations. Proceedings of MICCAI'99, Lecture Notes in Computer Science 1999;1679:788–97.

43. Sethian JA. A fast marching level set method for monotonically advancing fronts. Proc Natl Acad Sci USA 1996;93:1591–5.

44. Moshfeghi M, Ranganath S, Nawyn K. 3-Dimensional elastic matching of volumes. IEEE Trans Med Imaging 1994;3:128–38.

45. Davatzikos C, Prince JL, Bryan RN. Image registration based on boundary mapping. IEEE Trans Med Imaging 1996;15:112–5.

46. Ferrant M, Nabavi A, Macq B, Jolesz FA, Kikinis R, Warfield SK. Registration of 3-D intraoperative MR images of the brain using a finite-element biomechanical model. IEEE Trans Med Imaging 2001;20:1384–97.

47. Audette MA, Ferrie FP, Peters TM. An algorithmic overview of surface registration techniques for medical imaging. Med Image Anal 2000;4:201–17.

48. Roche A, Malandain G, Pennec X, Ayache N. The correlation ratio as a new similarity measure for multimodal image registration. Proceedings of MICCAI 1998, Lecture Notes in Computer Science 1998;1496:1115–24.

49. Collins DL, LeGoualher G, Venugopal R, Caramanos A, Evans AC, Barillot C. Cortical constraints for non-linear cortical registration. Visualization in Biomedical Computing, Lecture Notes in Computer Science 1996;1131: 307–16.

50. Hellier P, Barillot C. Coupling dense and landmark-based approaches for nonrigid registration. IEEE Trans Med Imaging 2003;22:217–27.

51. Liu TM, Shen DG, Davatzikos C. Deformable registration of cortical structures via hybrid volumetric and surface warping. NeuroImage 2004;22:1790–801.

52. Thompson PM, MacDonald D, Mega MS, Holmes CJ, Evans AC, Toga AW. Detection and mapping of abnormal brain structure with a probabilistic atlas of cortical surfaces. J Comput Assist Tomogr 1997;21: 567–81.

53. Christensen G, Carlson B, Chao KSC, Yin P, Grigsby PW, Nguyen K, et al. Image-based dose planning of intracavitary brachytherapy: registration of serial imaging studies using deformable anatomic templates. Int J Radiat Oncol Biol Phys 2001;51:227–43.

54. Russakoff DB, Rohlfing T, Shahidi R, Kim DH, Adler JR, Maurer CR. Intensity-based 2D-3D spine image registration incorporating one fiducial marker. Proceedings of MICCAI 2003 Part I, Lecture Notes in Computer Science 2003;2878:287–94.

55. Cachier P, Bardinet E, Dormont D, Pennec X, Ayache N. Iconic feature based nonrigid registration: the PASHA algorithm. Compu Vision Image Understanding 2003;89: 272–98.

56. Woods RP, Grafton ST, Watson JDG, Sicotte NL, Mazziotta JC. Automated image registration: II. Intersubject validation of linear and nonlinear models. J Comput Assist Tomogr 1998;22:153–65.

57. Bookstein FL. Principal warps – thin-plate splines and the decomposition of deformations. IEEE Trans Pattern Anal 1989;11:567–85.

58. DeQuardo JR, Keshavan MS, Bookstein FL, Bagwell WW, Green WDK, Sweeney JA, et al. Landmark-based morphometric analysis of first-episode schizophrenia. Biol Psychiatry 1999;45:1321–8.

59. Downhill JE, Buchsbaum MS, Wei TC, Spiegel-Cohen J, Hazlett EA, Haznedar MM, et al. Shape and size of the corpus callosum in schizophrenia and schizotypal personality disorder. Schizophr Res 2000;42:193–208.

60. Gharaibeh WS, Rohlf FJ, Slice DE, DeLisi LE. A geometric morphometric assessment of change in midline brain structural shape following a first episode of schizophrenia. Biol Psychiatry 2000;48:398–405.

61. Holden M, Schnabel JA, Hill DLG. Quantification of small cerebral ventricular volume changes in treated growth hormone patients using non-rigid registration. IEEE Trans Med Imaging 2002;21:1292–301.

62. Mattes D, Haynor DR, Vesselle H, Lewellen TK, Eubank W. PET-CT image registration in the chest using free-form deformations. IEEE Trans Med Imaging 2003;22:120–8.

63. Frangi AF, Rueckert D, Schnabel JA, Niessen WJ. Automatic construction of multiple-object three-dimensional statistical shape models: application to cardiac modelling. IEEE Trans Med Imaging 2002;21:1151–66.

64. McLeish K, Hill DLG, Atkinson D, Blackall JM, Razavi R. A study of the motion and deformation of the heart due to respiration. IEEE Trans Med Imaging 2002;21:1142–50.

65. Rohlfing T, Maurer CR, O'Dell WG, Zhong JH. Modeling liver motion and deformation during the respiratory cycle using intensity-based nonrigid registration of gated MR images. Med Phys 2004;31:427–32.

66. Schnabel JA, Tanner C, Castellano-Smith AD, Degenhard A, Leach MO, Hose DR, et al. Validation of non-rigid registration using finite element methods: application to breast MR images. IEEE Trans Med Imaging 2003;22:238–47.

67. Tanner C, Schnabel JA, Degenhard A, Castellano-Smith AD, Hayes C, Leach MO, et al. Validation of volume-preserving non-rigid registration: application to contrast-enhanced MR-mammography. Proceedings of MICCAI 2002, Lecture Notes in Computer Science 2002;2489:307–14.

68. Bajcsy R, Kovacic S. Multiresolution elastic matching. Comp Vision Graphics Image Processing 1989;46:1–21.

69. Christensen GE, Rabbitt RD, Miller MI. Deformable templates using large deformation kinematics. IEEE Trans Image Processing 1996;5:1435–47.

70. BroNielsen M, Gramkow C. Fast fluid registration of medical images. Visualization in Biomedical Computing, Lecture Notes in Computer Science 1996;1131:267–76.

71. Thirion J-P. Image matching as a diffusion process: an analogy with Maxwell's demons. Med Image Anal 1998;2:243–60.

72. Pennec X, Cachier P, Ayache A. Understanding the Demons' algorithm: 3D non-rigid registration by gradient descent. Proceedings of MICCAI 1999, Lecture Notes in Computer Science 1999;1679:597–605.

73. Hagemann A, Rohr K, Stiehl HS, Spetzger U, Gilsbach JM. Biomechanical modeling of the human head for physically based, nonrigid image registration. IEEE Trans Med Imaging 1999;18:875–84.

74. Dougherty L, Asmuth JC, Blom AS, Axel L, Kumar R. Validation of an optical flow method for tag displacement estimation. IEEE Trans Medl Imaging 1999;18:359–63.

75. Dougherty L, Asmuth JC, Gefter WB. Alignment of CT lung volumes with an optical flow method. Acad Radiol 2003;10:249–54.

76. Hayton PM, Brady M, Smith SM, Moore N. A non-rigid registration algorithm for dynamic breast MR images. Artificial Intelligence 1999;114:125–56.

77. Mori K, Deguchi D, Sugiyama J, Suenaga Y, Toriwaki J, Maurer CR, et al. Tracking of a bronchoscope using epipolar geometry analysis and intensity-based image registration of real and virtual endoscopic images. Med Image Anal 2002;6:321–36.

78. Fox NC, Crum WR, Scahill RI, Stevens JM, Janssen JC, Rossor MN. Imaging of onset and progression of Alzheimer's disease with voxel-compression mapping of serial MRI. Lancet 2001;358:201–5.

79. Besl PJ, McKay HD. A method for registration of 3-D shapes. IEEE Pattern Analysis Machine Intelligence 1992;14:239–56.

80. Chui HL, Rangarajan A. A new point matching algorithm for non-rigid registration. Comput Vision Image Understanding 2003;89:114–41.

81. Fitzgibbon AW. Robust registration of 2D and 3D point sets. Image Vision Comput 2003;21:1145–53.

82. Press WH, Teukolsky SA, Vetterling WT, Flannery BP. Numerical recipes in C. The Art of Scientific Computing. Cambridge, UK: Cambridge University Press, 1992.

83. Fitzpatrick JM, West JB. The distribution of target registration error in rigid-body point-based registration. IEEE Trans Med Imaging 2001;20:917–27.

84. Collins DL, Evans AC. Animal: validation and applications of nonlinear registration-based segmentation. Int J Pattern Recogn Artificial Intelligence 1997;11:1271–94.

85. Christensen GE, Johnson HJ. Invertibility and transitivity analysis for nonrigid image registration. J Electron Imaging 2003;12:106–17.

86. Sermesant M, Forest C, Pennec X, Delingette H, Ayache N. Deformable biomechanical models: Application to 4D cardiac image analysis. Med Image Anal 2003;7:475–88.

87. Rao A, Sanchez-Ortiz GI, Chandrashekara R, Lorenzo-Valdes M, Mohiaddin R, Rueckert D. Comparison of cardiac motion across subjects using non-rigid registration. Proceedings of MICCAI 2002 Part I, Lecture Notes in Computer Science 2002;2488:722–9.

88. Slomka PJ, Nishina H, Berman DS, Kang XP, Akincioglu C, Friedman JD, et al. "Motion-frozen" display and quantification of myocardial perfusion. J Nucl Med 2004;45:1128–34.

89. Blackall JM, King AP, Penney GP, Adam A, Hawkes DJ. A statistical model of respiratory motion and deformation of the liver. Proceedings of MICCAI 2001, Lecture Notes in Computer Science 2001;2208:1338–40.

90. Gee J, Sundaram T, Hasegawa I, Uematsu H, Hatabu H. Characterization of regional pulmonary mechanics from serial magnetic resonance imaging data. Acad Radiol 2003;10:1147–52.

91. Boldea V, Sarrut D, Clippe S. Lung deformation estimation with non-rigid registration for radiotherapy treatment. Proceedings of MICCAI 2003, Lecture Notes in Computer Science 2003;2878:770–7.

92. Fei B, Kemper C, Wilson DL. A comparative study of warping and rigid body registration for the prostate and pelvic MR volumes. Comput Med Imaging Graphics 2003;27:267–81.

93. Bharatha A, Hirose M, Hata N, Warfield SK, Ferrant M, Zou KH, et al. Evaluation of three-dimensional finite element-based deformable registration of pre- and intra-operative prostate imaging. Med Phys 2001;28:2551–60.

94. Schaly B, Kempe JA, Bauman GS, Battista JJ, Van Dyk J. Tracking the dose distribution in radiation therapy by accounting for variable anatomy. Phys Med Biol 2004;49:791–805.

95. Hohe J, Faber S, Muehlbauer R, Reiser M, Englmeier KH, Eckstein F. Three-dimensional analysis and visualization of regional MR signal intensity distribution of articular cartilage. Med Eng Phys 2002;24:219–27.

96. Bookstein FL. "Voxel-based morphometry" should not be used with imperfectly registered images. NeuroImage 2001;14:1454–62.

97. Ashburner J, Friston KJ. Why voxel-based morphometry should be used. NeuroImage 2001;14:1238–43.

98. Davatzikos C. Why voxel-based morphometric analysis should be used with great caution when characterizing group differences. NeuroImage 2004;23:17–20.

99. Lancaster JL, Fox PT, Downs H, Nickerson DS, Hander TA, El Mallah M, et al. Global spatial normalization of human brain using convex hulls. J Nucl Med 1999;40:942–55.

100. Good CD, Johnsrude IS, Ashburner J, Henson RNA, Friston KJ, Frackowiak RSJ. A voxel-based morphometric study of ageing in 465 normal adult human brains. NeuroImage 2001;14:21–36.

101. Baron JC, Chetelat G, Desgranges B, Perchey G, Landeau B, de la Sayette V, et al. In vivo mapping of gray matter loss with voxel-based morphometry in mild Alzheimer's disease. NeuroImage 2001;14:298–309.

102. Burton EJ, Karas G, Paling SM, Barber R, Williams ED, Ballard CG, et al. Patterns of cerebral atrophy in dementia with Lewy bodies using voxel-based morphometry. NeuroImage 2002;17:618–30.

103. Busatto GE, Garrido GEJ, Almeida OP, Castro CC, Camargo CHP, Cid CG, et al. A voxel-based morphometry study of temporal lobe gray matter reductions in Alzheimer's disease. Neurobiol Aging 2003;24:221–31.

104. Frisoni GB, Testa C, Zorzan A, Sabattoli F, Beltramello A, Soininen H, et al. Detection of grey matter loss in mild Alzheimer's disease with voxel based morphometry. J Neurol Neurosurg Psychiatry 2002;73:657–64.

105. Gee J, Ding LJ, Xie ZY, Lin M, DeVita C, Grossman M. Alzheimer's disease and frontotemporal dementia exhibit distinct atrophy-behavior correlates: a computer-assisted imaging study. Acad Radiol 2003;10:1392–401.

106. Merschhemke M, Mitchell TN, Free SL, Hammers A, Kinton L, Siddiqui A, et al. Quantitative MRI detects abnormalities in relatives of patients with epilepsy and malformations of cortical development. NeuroImage 2003;18:642–9.

107. Keller SS, Wieshmann UC, Mackay CE, Denby CE, Webb J, Roberts N. Voxel based morphometry of grey matter abnormalities in patients with medically intractable temporal lobe epilepsy: effects of side of seizure onset and epilepsy duration. J Neurol Neurosurg Psychiatry 2002;73:648–56.

108. Job DE, Whalley HC, McConnell S, Glabus M, Johnstone EC, Lawrie SM. Voxel-based morphometry of grey matter densities in subjects at high risk of schizophrenia. Schizophr Res 2003;64:1–13.

109. Pol HEH, Schnack HG, Mandl RCW, Cahn W, Collins DL, Evans AC, et al. Focal white matter density changes in schizophrenia: reduced inter-hemispheric connectivity. NeuroImage 2004;21:27–35.

110. Kochunov P, Lancaster J, Thompson P, Toga AW, Brewer P, Hardies J, et al. An optimized individual target brain in the talairach coordinate system. NeuroImage 2002;17:922–7.

111. Cootes TF, Marsland S, Twining CJ, Smith K, Taylor CJ. Groupwise diffeomorphic non-rigid registration for automatic model building. Computer Vision - ECCV 2004 Part 4, Lecture Notes in Computer Science 2004;2034:316–27.

112. Hill DLG, Hajnal JV, Rueckert D, Smith SM, Hartkens T, McLeish K. A dynamic brain atlas. Proceedings of MICCAI 2002 Part I, Lecture Notes in Computer Science 2002;2488:532–9.

113. Sonka M, Grunkin M. Image processing and analysis in drug discovery and clinical trials. IEEE Trans Med Imaging 2002;21:1209–11.

114. Meier DS, Guttmann CRG. Time-series analysis of MRI intensity patterns in multiple sclerosis. NeuroImage 2003;20:1193–209.

115. Bosc M, Heitz F, Armpspach JP, Namer I, Gounot D, Rumbach L. Automatic change detection in multimodal serial MRI: application to multiple sclerosis lesion evolution. NeuroImage 2003;20:643–56.

116. Hartkens T, Hill DLG, Castellano-Smith AD, Hawkes DJ, Maurer CR, Martin AJ, et al. Measurement and analysis of brain deformation during neurosurgery. IEEE Trans Med Imaging 2003;22:82–92.

117. Davis MH, Khotanzad A, Flamig DP, Harms SE. A physics-based coordinate transformation for 3-D image matching. IEEE Trans Med Imaging 1997;16:317–28.

118. Bruckner T, Lucht R, Brix G. Comparison of rigid and elastic matching of dynamic magnetic resonance mammographic images by mutual information. Med Phys 2000;27:2456–61.

119. Rohlfing T, Maurer CR Jr, Bluemke DA, Jacobs MA. Volume-preserving nonrigid registration of MR breast images using free-form deformation with an incompressibility constraint. IEEE Trans Med Imaging 2003;22:730–41.

120. Xiao GF, Brady JM, Noble JA, Burcher M, English R. Nonrigid registration of 3-D free-hand ultrasound images of the breast. IEEE Trans Med Imaging 2002;21:405–12.

121. Shen DG, Herskovits EH, Davatzikos C. An adaptive-focus statistical shape model for segmentation and shape modeling of 3-D brain structures. IEEE Trans Med Imaging 2001;20:257–70.

122. Marroquin JL, Vemuri BC, Botello S, Calderon F, Fernandez-Bouzas A. An accurate and efficient Bayesian method for automatic segmentation of brain MRI. IEEE Trans Med Imaging 2002;21:934–45.

123. Klemencic J, Pluim JPW, Viergever MA. Non-rigid registration based active appearance models for 3D medical image segmentation. J Imaging Sci Technol 2004;48:166–71.

124. Crum WR, Scahill RI, Fox NC. Automated hippocampal segmentation by regional fluid registration of serial MRI: validation and application in Alzheimer's disease. NeuroImage 2001;13:847–55.

125. Park H, Bland PH, Meyer CR. Construction of an abdominal Probabilistic atlas and its application in segmentation. IEEE Trans Med Imaging 2003;22:483–92.

126. Noble NMI, Hill DLG, Breeuwer M, Schnabel JA, Hawkes DJ, Gerritsen FA, et al. Myocardial delineation via registration in a polar coordinate system. Acad Radiol 2003;10:1349–58.

Appendix 1

Terminology

The registration community use a number of terms for the same things that can confuse the unwary. When two images are being registered one is conventionally regarded as static and defining a frame of reference and the other is transformed (*i.e.* translated, rotated, scaled, sheared, warped) to bring corresponding features into alignment. The static image is variously known as the target, reference or baseline image. The image undergoing transformation is then known as the source, floating or repeat image. The criterion used to register two images can be known as the similarity measure or the objective or cost function. The geometrical transformation that maps features in one image to features in another is known as the transformation, deformation field, displacement field or warp. These transformations are usually classified as being rigid, affine or non-rigid. The terms "linear" and "non-linear" are sometimes substituted for affine and non-rigid although this is not strictly correct. Other common terms that are often used together are homology (as in the homologues of Richard Owen, the famous anatomist of the 19th century) and correspondence errors. The TRE, a short-hand for target registration error, is often quoted to give an idea of the mean registration error in an image. In some cases this can be calculated explicitly but this is usually not the case for prospective non-rigid registration.

In this paper we will register "source" images to "target" images usually by maximizing a "similarity measure" resulting in a "deformation" field. We will also talk generally about "transformations" when appropriate. See Figure 1 for an example of image registration.